Changes in Membrane Properties during Energy Depletion-Induced Cell Injury Studied with Fluorescence Microscopy

Yankuan Wu,* Frank F. Sun,* Donald M. Tong,# and Bruce M. Taylor*
*Cell Biology and Inflammation Research and #Biostatistics and Clinical Data Management, Pharmacia and Upjohn, Kalamazoo, Michigan 49001 USA

ABSTRACT The changes in membrane structural properties occurring during the process of ATP depletion-induced cell injury in adherent human astrocytoma cells (UC-11 MG) were studied with two epifluorescence techniques: 1) steady-state fluorescence anisotropy (r) to examine microstructural changes in the membrane phospholipids and 2) fluorescence redistribution after photobleaching (FRAP) to examine membrane fluidity changes. A new method for r measurement was established that provides the unique advantage of simultaneously monitoring both vertical and horizontal polarized fluorescence emissions needed for the calculation of r. In this study, r in the astrocytoma cells labeled with 1-(4-trimethylammonium phenyl)-6-phenyl-1,3,5-hexatriene p-toluenesulfonate was shown to remain stable for up to 90 min. However, when the cells were treated with 75 μM iodoacetic acid (IAA), a metabolic inhibitor that induces rapid depletion of cellular ATP, r continually decreased, indicating a decrease in membrane lipid order and perturbation of the bilayer structure. This decrease in r could be prevented by the pretreatment of cells with lipophilic antioxidants such as tirilazad or gossypol. Tirilazad itself caused a significant increase in r, suggesting that tirilazad intercalates into the membrane bilayer and profoundly increases the lipid order in uninjured cells. Gossypol, however, did not exhibit this property. Further investigations into these phenomena with FRAP confirmed the r results and indicated that membrane fluidity increased while its structure became less rigid during the process of ATP-induced cell injury. In addition, lipophilic antioxidants prevented the membrane structural aberrations induced by IAA. Experimental results suggest that different mechanisms of cytoprotective action may exist for tirilazad and the antioxidant gossypol. Gossypol appears to prevent or delay the observed cell injury entirely because of its antioxidant action, whereas tirilazad's protection is mediated not only via its antioxidant activity, but also by its ability to increase cell membrane lipid order.

INTRODUCTION

Decreased cellular ATP is one of the major biological events occurring immediately after the onset of ischemic tissue injury (Farber et al., 1981; Jennings and Reimer, 1981; Raichle, 1983). If the noxious conditions persist, a cascade of biological events occurs within cells that leads to irreversible injury and eventually to cell death. There is increasing evidence implicating alterations in the physical state of the biological membrane as a major factor in the evolution of irreversible injury during cellular ATP depletion (Florine-Casteel et al., 1991). Many methods have been developed and applied to study of the changes in membrane structure during the cell injury process, including fluorescence microscopy, which has been widely used in biological systems (Lakowicz, 1991; Taylor and Wang, 1989; Wang and Taylor, 1989).

Two techniques, fluorescence redistribution after photobleaching (FRAP), which can be used to measure the diffusion coefficient of a fluorescent probe within the membrane, and steady-state fluorescence anisotropy (r), which can be used to monitor the motion of fluorophores in living cell membranes, have been employed for the study of structural changes within a cell membrane. Fluorescence anisotropy involving measurement of the polarized emissions of a fluorophore in the membrane can provide a detailed description of the rotational motion of a fluorophore and, thus, be used to characterize the microviscosity of the environment surrounding the fluorophore. Typically, very rigid structures exhibit a larger r value than more fluid structures. In contrast, FRAP utilizes fluorescent phospholipid analogs to reveal membrane lipid structural changes by measuring the diffusion coefficients of the fluorescent probes. Collective results from both r and FRAP measurements can provide profound insight into structural changes within the cell membranes. Through the use of these techniques, internal movements of the macromolecules in the membrane can be monitored, allowing examination of the nature of the microenvironment surrounding the fluorescent probes.

Most of the applications involving anisotropic measurements have been made in lipid vesicles or cell systems in suspension (Collins and Grogan, 1989; Sawyer, 1988).

However, it is likely that important information about the cells may be lost after dissociation of the cells from their living substrate. Recently, quantitative fluorescence imaging has been used to provide spatially resolved images reflecting r and the diffusion coefficient of fluorophores within plasma membranes and in the cytoplasm of adherent cells (Dix and Verkman, 1990; Gough and Taylor, 1993; Schindler and Jiang, 1987).

Received for publication 6 May 1994 and in final form 12 April 1996.

Address reprint requests to Bruce M. Taylor, Cell Biology and Inflammation Research, PNU, Kalamazoo, MI 49007. Tel.: 616-833-7752; Fax: 616-833-9324; E-mail: bmtaylor@pwinet.upj.com.

Dr. Wu's present address is The Upjohn Company, Room 10014, CATIC Plaza Office Blvd., Bei Chen East Rd. no. 18, Chaoyang District, Beijing 100101, People's Republic of China.

0006-3495/96/07/91/10 $2.00

Here, we report the establishment of a new methodology for the measurement of steady-state fluorescence anisotropy that exhibits the unique advantage of simultaneously monitoring both the vertical (parallel) and the horizontal (perpendicular) polarized fluorescence emissions while automatically correlating the ratio of the emissions to r. This method was utilized in the present study to measure the changes in r within the membranes of adherent human astrocytoma cells during the process of ATP depletion-induced cell injury and to investigate the ability of antioxidants to prevent these changes. In addition, changes in the diffusion coefficients within the membranes were measured with FRAP to confirm the results of the r measurements.

MATERIALS AND METHODS

Materials

RPMI 1640 cell culture medium, HEPES buffer, and Hanks' balanced salt solution (HBSS) were obtained from Gibco BRL (Grand Island, NY). Iodoacetic acid (sodium salt), 2,2′-bi(8-formyl-1,6,7-trihydroxy-5-isopropyl-3-methylnaphthalene (gossypol), and bovine serum albumin were purchased from Sigma Chemical Company (St. Louis, MO). Tirilazad mesylate (U-74006F) was provided by Dr. Gordon L. Bundy of Medicinal Chemistry Research, Upjohn Laboratories. Fluorescent probes, 1-(4-trimethylammonium phenyl)-6-phenyl-1,3,5-hexatriene *p*-toluenesulfonate (TMA-DPH) and 2-(6-(7-nitrobenz-2-oxa-1,3-diazol-4-yl)amino)hexanol-1-hexadecanoyl-sn-glycero-3-phosphocholine (NBD-PC), were purchased from Molecular Probes (Eugene, OR). Lab-Tek coverglass chambers for tissue culture were obtained from Nunc (Naperville, IL).

Cell culture and preparation

The human astrocytoma cell line, UC-11 MG, was kindly provided by Dr. Thomas J. Raub of Drug Delivery Research, Upjohn Laboratories. Cells were grown in 75-cm^2 culture flasks with RPMI 1640 culture medium containing 4 mM L-glutamine, 20 mM HEPES, 10% fetal bovine serum, penicillin, streptomycin, and amphotericin B. Cultures were incubated at 37°C in a humidified atmosphere containing 5% CO_2. On the day before the experiment cells were seeded at $5 \times 10^4/cm^2$ into two- or four-well Lab-Tek chambers that had been etched with NaOH (1 M) and coated with collagen (Type I rat tail collagen at 1:20 dilution of stock solution; Collaborative Research, Bedford, MA). Astrocytes were pretreated with gossypol and tirilazad, which were prepared as 0.01 M and 0.1 M stock solutions, respectively, in dry dimethylsulfoxide (DMSO) and diluted 1:10 in 30 mg/ml bovine serum albumin solution. The 100× compound solutions were prepared by diluting the above solution 1:10 with HBSS containing Ca^{2+} and Mg^{2+}, 1.2 and 0.8 mM, respectively (complete HBSS). These concentrated drug solutions were added to the cells in culture medium to yield final concentrations of 1 μM for gossypol and 10 μM for tirilazad. The cells were preincubated for 2 h at 37°C before initiation of cell injury.

Imaging and data processing

All quantitative fluorescence measurements were conducted with an ACAS 570 interactive laser cytometer. This working station utilizes an Olympus inverted microscope coupled to an argon laser that is tunable to UV (351–364 nm) and several useful visible wavelengths (488 and 514 nm) for the excitation of a variety of fluorescent probes. As shown in Fig. 1, it is equipped with two photomultiplier tube (PMT) detectors, which enable simultaneous ratio imaging. Data collected was normalized to correct for background:

$$\text{Normalization} \quad \text{Val}(t)/\text{Val}(t = 0),$$

where Val(t) is the observed fluorescence at the time indicated and Val(t = 0) is the observed fluorescence at the time of the first reading (time 0).

Cell injury assay

Sodium iodoacetate (IAA) (75 μM) was used to deplete cellular ATP in all cell injury assays. Adherent human astrocytoma cells in the coverslip chambers were washed once with warm, complete HBSS before use. Then complete HBSS containing 75 μM IAA was added to the culture chamber to induce cell injury. For cytoprotective experiments, gossypol or tirilazad, at indicated concentrations, was present during the entire assay period. All experiments were conducted at 37°C, using a temperature-controlled stage on a confocal ACAS 570 interactive laser cytometer (Meridian Instruments, Okemos, MI).

Steady-state fluorescence anisotropy measurements

For steady-state fluorescence anisotropy measurements, adherent cells were washed once with complete HBSS and then incubated in this medium containing 2 μM TMA-DPH for 10 min at 37°C. After this incubation, the cells were washed once with complete HBSS and imaged using an ACAS interactive laser cytometer.

The fluorescent probe was excited using the coherent UV band (351–364 nm) of a 5-W argon laser (Coherent, I-90). The polarized UV light was directed through an acoustooptic modulator (AOM), which controls the laser's spot intensity and pulse duration, and then through a 355/30-nm band-pass excitor filter. The UV light was reflected through the center of a UV-quality objective (Olympus X UV Dapo objective; NA = 1.30) using a 380-nm long-pass dichroic filter. Fluorescence emissions from the sample returned through the objective, passed through the 380-nm long-pass dichroic filter, and then through a 390-nm long-pass barrier filter. A 50/50 beam splitter positioned after a pinhole aperture was used to direct half of the fluorescence emission through a vertically polarized filter to a PMT detector, and half of the fluorescence emission through a horizontally polarized filter to a second PMT detector (Fig. 1). Imaging was typically performed using 0.1% of the laser light when its output was set at 100 mW.

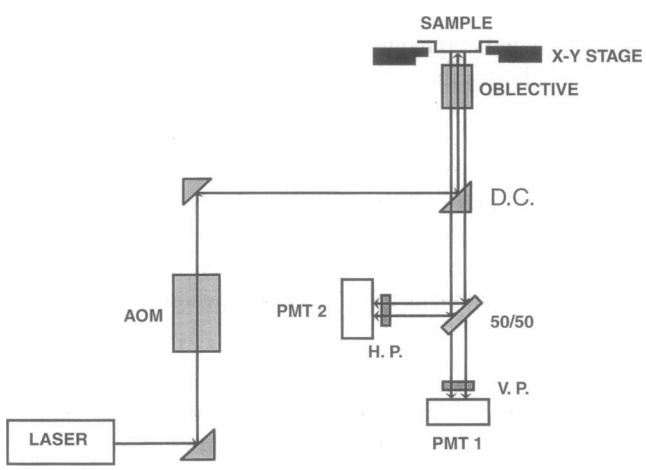

FIGURE 1 Schematic diagram for measurement of steady-state fluorescence anisotropy in the ACAS interactive laser cytometer. V.P., Vertical polarizer; H.P., horizontal polarizer; D.C., dichroic cube containing a 355/30-nm band pass excitation filter, a 380-nm long-pass dichroic filter, and a 390-nm long-pass barrier filter; AOM, acousto-optic modulator.

Using a motorized stage, the samples were scanned point by point in the x and y directions over the stationary laser beam. Stage scanning in such a manner eliminates many of the imaging artifacts that result from scanning a laser beam across the objective lens. To reduce axial UV chromatic error in the objective, a beam expander in the ACAS 570 is employed in the excitation beam to adjust its focus. The visible fluorescence path is unmodified, and so is not affected by the UV correction. A typical image of 180 × 180 pixels at the step size of 1 μ per pixel (imaging area is 180 μ × 180 μ) was scanned within 30 s. To determine distribution of the TMA-DPH probe within the cellular environment, a confocal scan was prepared of a labeled cell. For the confocal imaging 160 × 160 pixels were scanned in the x-y plane, using a step size of 0.3 μm and a pinhole setting of 100 μm. Scans were repeated every 0.5 μm in the z plane to compile data for three-dimensional reconstruction of the image. It should be noted that theoretical resolution for fluorescence imaging using this pinhole setting and UV excitation with the 1.30 NA objective is 0.53 μm. Therefore, acquisition of 0.5-μm sections during confocal imaging means sampling at or slightly below the optimal resolution of the instrument.

With the split emission light and dual PMTs described above, r was calculated from the fluorescence emissions as follows:

$$r = (I_v - g*I_h)/(I_v + 2g*I_h) = (A - g)/(A + 2g),$$

where I_v and I_h are the vertical and horizontal fluorescence intensities measured by detectors 1 and 2, respectively, g is a factor that corrects for differential polarization sensitivity of the detection system (Lakowicz, 1983), and A equals the ratio of the two emissions, I_v/I_h. Factor g is set to 1 by adjusting the PMT gains until the emitted fluorescence intensities displayed by each detector are approximately equal when the 50/50 beam splitter was used alone, but without the vertical and horizontal polarizing filters. The ACAS automatically converted the ratio A to r using a build-in standard curve. Background autofluorescence was removed by subtracting the fluorescence image acquired before staining from the fluorescence images of the same field acquired after staining with TMA-DPH.

The accuracy of the ACAS r measurements was determined by comparing the values recorded by the ACAS to the values measured using a spectrofluorometer (ISS Instruments, Urbana, IL). The comparisons were conducted on cell-free DMSO solutions containing 1 μM TMA-DPH and 1–76% glycerol, used to control the fluid viscosity.

Diffusion coefficient measurements

Measurement of fluorescence redistribution after photobleaching (FRAP) was used to investigate membrane fluidity changes in human astrocytoma cells undergoing ATP depletion-induced cell injury. Adherent cells were washed once with complete HBSS and then labeled with 10 μg/ml of NBD-PC in complete HBSS at 37°C for 5 min. After incubation, excess fluorescent probes were removed by rinsing with complete HBSS.

FRAP measurements were performed with the ACAS by photobleaching a microscopic area (1.3 μm in diameter with a 40× Olympus LWD objective, NA 0.55) of a cell membrane using a short, intense pulse of laser light, controlled by the AOM. Typically, a 40-ms pulse of the 488-nm laser line, using 100% of the laser's 100-mW output, caused the fluorescence in the photobleached area to decrease by approximately 65%.

Fluorescence recovery within the bleached area due to the lateral diffusion of neighboring intact fluorophores was subsequently measured via a single line scan across the entire cell, including the bleached area, using the 488-nm laser attenuated to a lower scan strength. Typically, 30 μ line scans across a cell were recorded every second, using 5% laser scan strength (100 mW laser output). NBD-PC fluorescence recovery in the human astrocytoma cells was generally completed within 45 s.

The ACAS software automatically calculated the percent fluorescence recovery and the diffusion coefficient (cm^2/s) for the probe within the membrane, using a modified nonlinear least-squares algorithm for flat cells (Axelrod et al., 1976; Golan et al., 1986). For each series of experiments, the calculated diffusion coefficients were compared by performing a one-way ANOVA. Comparisons between experimental groups were performed using the F-folded test (SAS Version 6.8) at specific time points. All differences that reached a probability of 5% or less were considered statistically significant.

Determination of cell viability

Propidium iodide (PI) was utilized to monitor viability in the cell injury experiments. This probe is excluded from viable cells, where it exhibits very little fluorescence; however, as the cells were injured and lost their membrane permeability barrier, propidium iodide entered the cell binding to nucleic acids to become highly fluorescent. Propidium iodide at a final concentration of 10 μM was added to the culture chamber just before cell injury induction. The fluorophore was excited at 488 nm and the emission fluorescence was detected by PMT 2 with the 575-nm short-pass dichroic mirror and a 530 ± 30-nm band-pass filter.

RESULTS

Validation of steady-state fluorescence anisotropy with imaging technique

To validate the measurements of steady-state fluorescence anisotropy using the ACAS, a series of glycerol/DMSO solutions containing 1 μM TMA-DPH were analyzed using both the ACAS and a spectrofluorometer. The fluid viscosity was gradually increased in the solution by raising the percentage of glycerol. Theoretically, as the fluid viscosity of a solution is increased, r should increase proportionally. The linear relationship found between r measured with the spectrofluorometer and r measured by the ACAS indicates that measurements made with the two instruments are well correlated (Fig. 2). These results showed that r can be measured accurately with the ACAS.

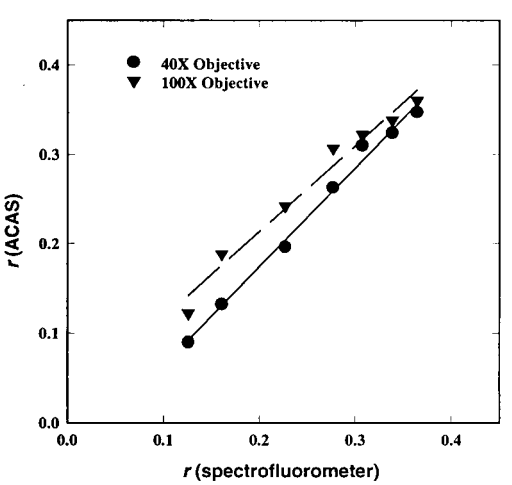

FIGURE 2 Comparison of steady-state fluorescence anisotropy measured by the ACAS versus the r measured by a spectrofluorometer using a series of glycerol/DMSO solutions containing 1 μM TMA-DPH. The viscosities of the bulk solutions were determined by the percentage of glycerol in each solution ranging from 1% to 76% (w/w). No significant depolarization in r by high numeric aperture of a 100× UV objective (▼) was observed by comparing with the r measured through a 40× UV objective (●).

Changes of steady-state fluorescence anisotropy by the treatment of lipophilic antioxidants

Steady-state fluorescence anisotropy within adherent human astrocytoma cells was determined by simultaneously monitoring horizontally and vertically polarized fluorescence emissions from the fluorescent probe TMA-DPH using the ACAS. A typical set of fluorescence images for the r measurement is shown in Fig. 3. The upper panel of Fig. 3 shows pseudocolor images of the distribution of the two polarized emissions in astrocytoma cells. Detector 1 represents the emission fluorescence intensity in the plane parallel to that of the excitation beam's (I_v) polarization, and detector 2 represents the emission fluorescence intensity in the plane perpendicular to that of the excitation beam's (I_h) polarization. The spatial distribution of r within the human astrocytoma cells, calculated from the ratio of the two emissions using the standard curve, is shown in the lower panel of Fig. 3 along with the corresponding pixel histogram. The limited range of r (0 to 0.5) agrees with

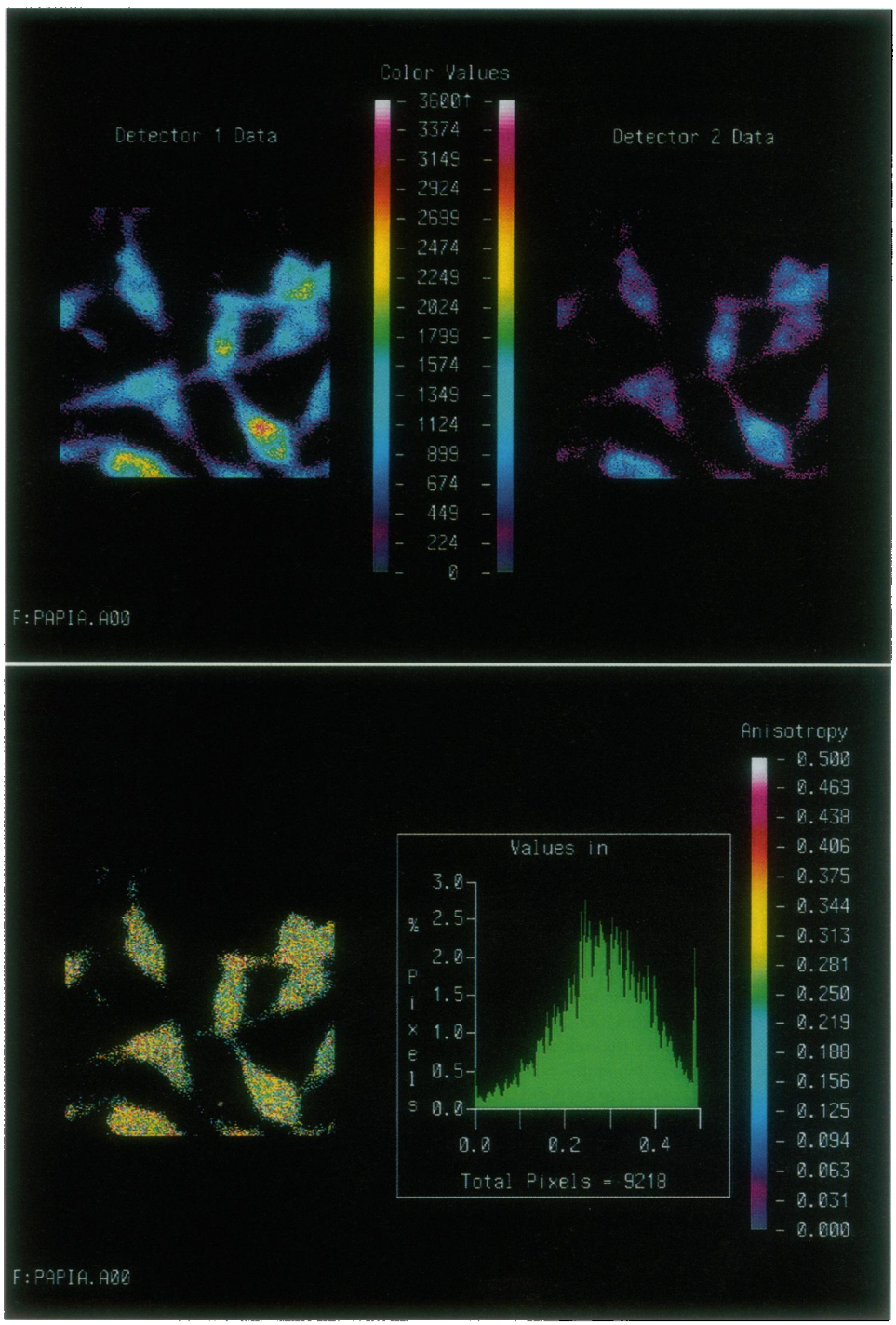

FIGURE 3 (*Top*)Pseudocolor images of the vertical polarized fluorescence emission (*left*) and the horizontal polarized fluorescence emission (*right*) from human astrocytoma cells loaded with 2 μM TMA-DPH. (*Bottom*) Pseudocolor image representing the spatial distribution of steady-state fluorescence anisotropy within human astrocytoma cells with the corresponding pixel histogram of r values. The r values are indicated by the adjacent color scale.

theoretical r values predicted for the biological systems (Lakowicz, 1983). The heterogeneity of r observed throughout each of the cells is probably due to structural differences in the lipid bilayer of each cell and/or to the internalization of fluorescent probes.

Control experiments were run to monitor the effect of laser excitation on the TMA-DPH probe and/or the membrane of the human astrocytoma cells over a long period of time where cells were incubated in complete HBSS alone. The results, shown in Fig. 4, indicate that r in the adherent cells remained constant for at least 1 h and then exhibited an insignificant decrease, which was probably due to internalization of fluorophores. Thus, any significant deviation in r from the control values should reflect changes in cell membrane structures.

Fig. 4 shows the changes of steady-state fluorescence anisotropy with time in human astrocytoma cells during the exposure to different lipophilic antioxidants. When the cells were treated with 1 μM gossypol, r decreased slightly and then stayed at a constant level, which was not significantly different than that of the original value ($t = 0$). Because the decrease in r occurred early in the antioxidant treatment, the small change was probably induced by the incorporation of gossypol into the cell membranes. Once the incorporation process reached a dynamic equilibrium, the overall membrane structure stayed at a relatively stable stage, as reflected by the constant r. In contrast, treatment of astrocytoma cells with 10 μM tirilazad induced an increase in r, which reached a maximum value in 30 min; that value differed significantly from that of the control cells. This increase in r indicates that significant structural changes in the membrane occurred upon tirilazad addition, resulting in a more rigid membrane environment.

Changes in steady-state fluorescence anisotropy during ATP depletion-induced cell injury

IAA is a metabolic inhibitor that induces cellular ATP depletion and irreversibly injures cells (Florine-Casteel et al., 1991; Sun et al., 1993). Fig. 5 shows the changes in steady-state fluorescence anisotropy (r) that occur in human astrocytoma cells during exposure to IAA (final concentration of 75 μM). The study revealed a steady decrease in r within the cells over the first hour, which then accelerated, suggesting that membrane structure was being altered to yield a more fluid microenvironment in the membrane bilayer.

However, when astrocytoma cells were pretreated for 2 h with lipophilic antioxidants before exposure to IAA, a de-

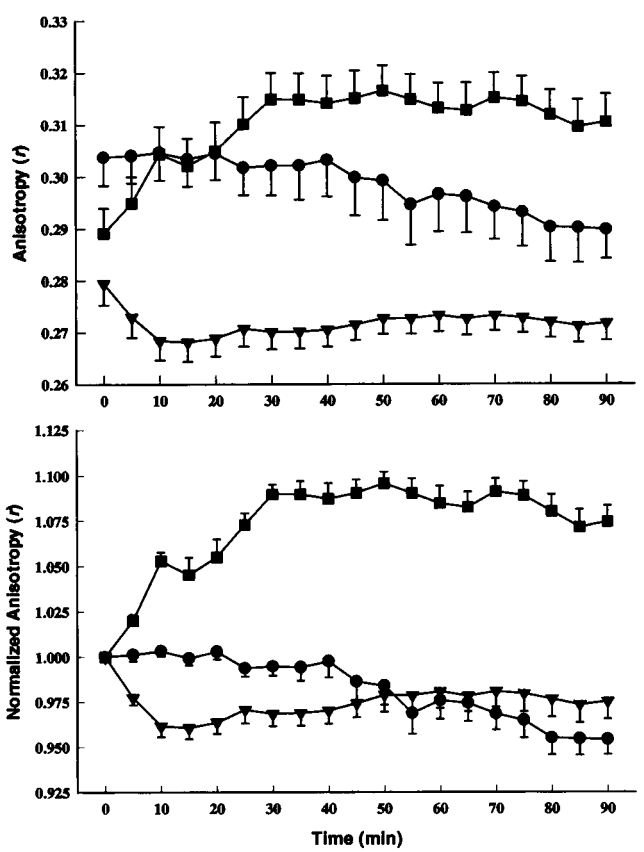

FIGURE 4 Time courses of steady-state fluorescence anisotropy (*top*) and normalized r (*bottom*) in human astrocytoma cells labeled with TMA-DPH under different treatments: ●, control; ■, 10 μM tirilazad; ▼, 1 μM gossypol. Values are mean ± SEM (n = 30–40 cells).

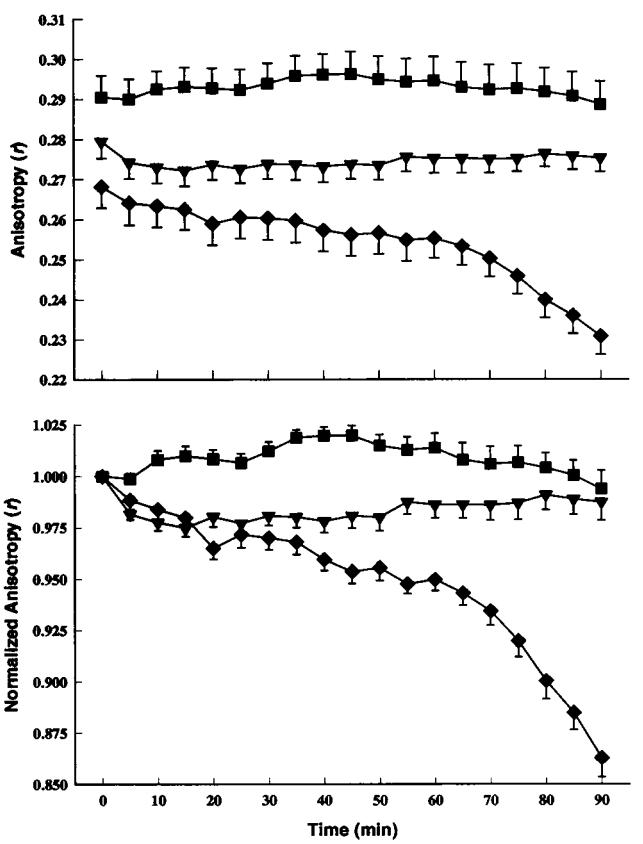

FIGURE 5 Changes in steady-state fluorescence anisotropy in the ATP-depleted human astrocytoma cells induced by IAA (◆) and the protective effect of the antioxidants (■, 10 μM tirilazad + IAA; ▼, 1 μM gossypol + IAA). (*Top*) Changes in r. (*Bottom*) Normalized changes in r. Values are mean ± SEM (n = 30–40 cells).

crease in r during IAA exposure was not observed (Fig. 5). In ATP-depleted cells that had been pretreated with 1 μM gossypol, a small decrease in r was observed immediately after the addition of IAA, similar to that seen initially during the gossypol treatment; however, r stayed constant thereafter at a level that was not significantly different from that of the undamaged cells when analyzed via Dunnet's t-test. In cells pretreated with 10 μM tirilazad before the addition of IAA, no significant changes in r were recorded during IAA treatment. These results suggest that the incorporation of antioxidants in the membrane bilayer prevents the membrane structural damage and increased fluidity that normally result from ATP depletion-induced cell injury.

To determine the amount of internalization of the TMA-DPH probe used for measurement of r, astrocytoma cells were loaded with the probe and dual-detector confocal sections through the cell were examined. Confocal imaging allows optical sectioning of the cell in the vertical plane (z axis) with a resolution of 0.53 μm, when a 100× objective is employed. Through the use of this extremely narrow depth of field, it was possible with the confocal system to establish three-dimensional localization of subcellular structures. Fig. 6 presents these confocal sections, which were taken through the center of the cell; the top image depicts a control cell after loading for 2 h with TMA-DPH, and the bottom image is of a cell preloaded for 4 h with tirilazad and then, as in the top figure,

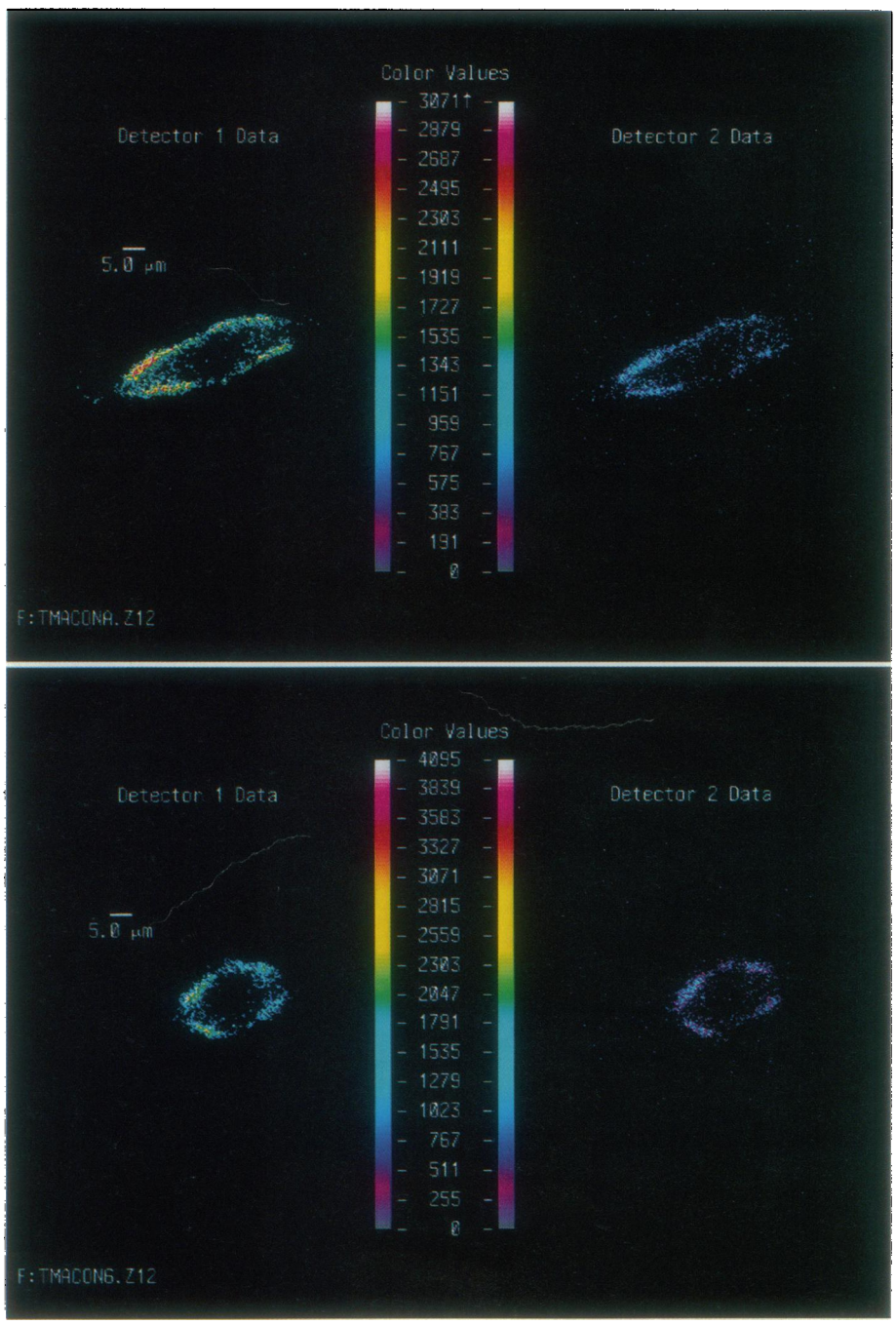

FIGURE 6 Pseudocolor images of confocal sections through the center of a TMA-DPH loaded astrocytoma cell probe distribution through the cell (detectors 1 and 2 are each detecting light in only one plane, horizontal or vertical). (*Top*) Cells labeled for 2 h with TMA-DPH. (*Bottom*) Effect of 4 h of preloading with tirilazad before the addition of TMA-DPH.

with TMA-DPH (detectors 1 and 2 are each detecting light in only one plane, horizontal or vertical). As indicated by these figures, most of the fluorophore is localized in the outer membrane, and therefore, changes in fluorescence polarization can be taken to reflect the state of the cell membrane. These images clearly indicate that the TMA-DPH is in or near the outer membrane, because the interior of the cell is devoid of the probe. The images presented in Fig. 3, in contrast to those presented here (Fig. 6), are of overall fluorescence of the TMA-DPH (epifluorescence), which provides no vertical resolution, and the probe, therefore, appears to be detected throughout the cell. Furthermore, tirilazad has very little, if any, effect on the anisotropy probe in these cells.

Membrane fluidity changes during ATP depletion-induced cell injury

Because membrane fluidity is proportionally related to the diffusion coefficient of fluorescent probe in the membrane, FRAP was utilized to corroborate the membrane fluidity changes detected in the human astrocytoma cells by the fluorescence anisotropy measurements during cell injury induced by ATP depletion. Fig. 7 shows the changes in NBD-PC probe diffusion coefficient (shown as mobility) in the cell membrane during the cell injury process. Each time point in Fig. 7 reflects the averaged value of diffusion coefficients in 10–20 individual cells. Unprotected cells exposed to 75 μM IAA showed a significant increase in membrane fluidity before 90 min. After 90 min, the injured cells partially detached from the bottom of the culture chamber, which made the measurements inaccurate and inconsistent. However, in cells pretreated for 2 h with antioxidants such as gossypol or tirilazad, the diffusion coefficient of NBD-PC is slower than, but insignificantly different from, the initial values observed in the control cells. When the antioxidant-pretreated cells were exposed to IAA, the diffusion coefficient of NBD-PC increased with time, but at a significantly slower rate than that of cells treated with IAA. These results indicate that the membrane structure in human astrocytoma cells is altered, shifting to a more fluid phase during periods of ATP depletion, and that this structural change may be attenuated by treatment with antioxidants.

Determination of cell viability during ATP depletion-induced cell injury

To establish whether a correlation exists between the observed changes in the membrane structure and cell viability, propidium iodide (PI) exclusion experiments were performed to detect the loss of the cell's permeability barrier. Propidium iodide, which is excluded from living cells, was added to the incubation buffer, where it exhibits low levels of fluorescence. As the cells lose viability after IAA treatment and the membrane permeability barrier disintegrates, PI enters the cell and binds with nucleic acids to become highly fluorescent (Goes et al., 1988; Nieminen et al., 1988). The data, which represent the mean of five groups of cells repeatedly scanned over the entire experimental period, are presented in Fig. 8. The results show that the unprotected cells lost their permeability barrier after 100 min of IAA treatment. As they died, there was an observed

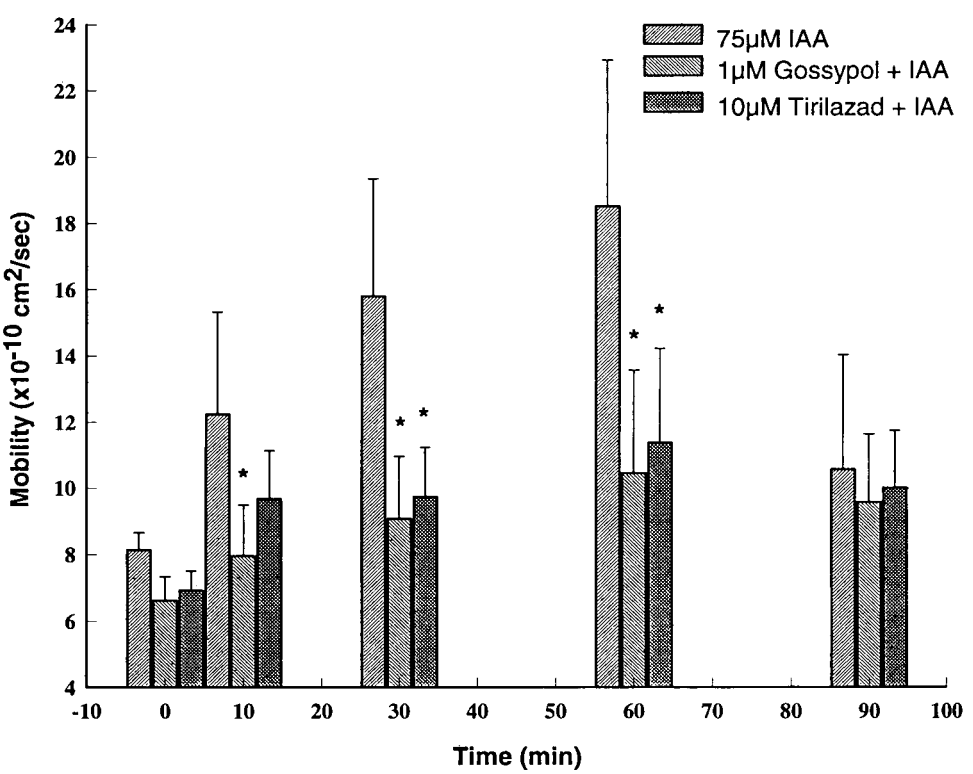

FIGURE 7 Changes in membrane fluidity, indicated by the fluorophore mobility measured from FRAP, occurring in the process of ATP depletion-induced cell injury in human cell astrocytoma cells. Lipophilic antioxidants demonstrated a strong protective effect (*, $p < 0.05$) at a certain time point when compared with the group treated with IAA alone. Values are mean ± SEM (n = 17–20 cells).

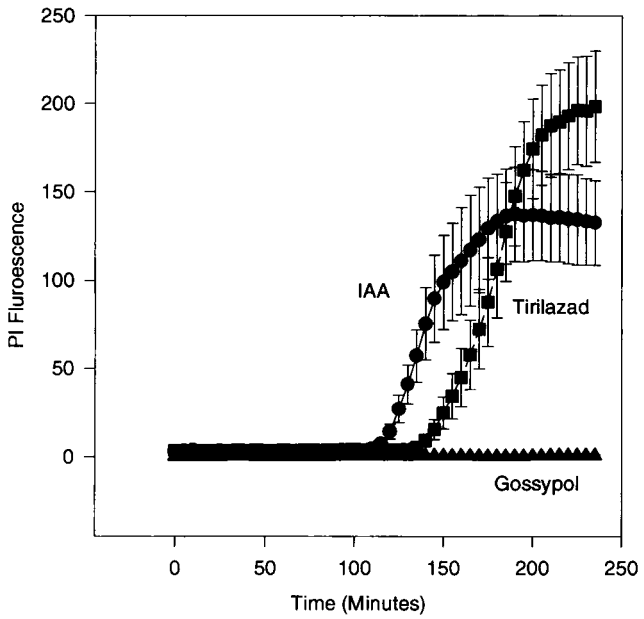

FIGURE 8 Effect of the antioxidants (■, 10 μM tirilazad; ▼, 1 μM gossypol) on 75 μM iodoacetate (●)-induced loss of cellular viability as monitored by prevention of propidium iodide (PI) entry into the cell, indicated by increases in intracellular PI fluorescence.

decline in PI fluorescence, which may have resulted from a loss of nucleic acids from the cells as the membrane became permeable and from a loss of cells as they floated off the culture plate, which resulted in an observed decrease in total PI fluorescence with long-term observation. These caused the decrease in intracellular fluorescence and introduced a high degree of variability, which is reflected in the large error bars at the later time points in Fig. 8. Gossypol completely protected the cells against IAA-induced injury for at least 4 h. Tirilazad was able to postpone cell death for approximately 45 min and decreased leakage of the PI probe from the cytoplasm, which accounts for the elevated intracellular fluorescence in the tirilazad-protected cells.

DISCUSSION

In the present study, a quantitative imaging fluorescence technique was developed to measure the steady-state fluorescence anisotropy of fluorescent probes in the membranes of human astrocytoma cells injured by ATP depletion. This imaging technique utilizes an argon laser as a source of polarized excitation light and two photomultiplier tubes to simultaneously record the polarized emission images, which were subsequently utilized to correlate the emission ratio with r. The results demonstrate that although the r values are slightly reduced in the imaging measurements, they strongly correlate with the values obtained from spectrofluorometer measurements and, therefore, can be correlated to the true values of r in living cell systems. This correlation was further confirmed by the data shown in Fig. 3, in which the limited range of r across the cells is in good agreement with the theoretically predicted values in biological systems (Lakowicz, 1991). Current techniques in which r is measured in different adherent living cell systems, as reported by a number of investigators (Wang et al., 1995; Fushimi et al., 1990; Florine-Casteel et al., 1991; Gough and Taylor, 1993), all use one imaging detector in their optical system, requiring sequential recording of the polarized emissions. This type of imaging may result in the loss of useful information due to the process of changing optics in the light pathway when living cells are monitored. The method described in this report has some unique advantages: 1) the vertical and horizontal polarized fluorescence emissions can be simultaneously monitored to acquire the r measurements for an entire cell or a group of cells, and 2) the time course of r changes in the same cell can be observed for a long period of time, thus allowing calculation of normalized changes in r, which can be meaningfully interpreted as structural changes in cell membranes.

Iodoacetate has been shown to block glycolysis through the inhibition of glyceraldehyde 3-phosphate dehydrogenase in isolated perfused hearts (Padieu and Mommaerts, 1960; Pirolo and Allen, 1986; Jennings et al., 1989). This specificity has also been demonstrated in rat lung carcinoma cells (Brodie and Reed, 1987). At the 75 μm concentration employed in these studies, Dawson et al. (1993) have shown glyceraldehyde 3-phosphate dehydrogenase to be the main site of action for this alkylating agent. As a result of this inhibition, cellular ATP is rapidly depleted (Sun et al., 1993). IAA has been widely used to induce the condition termed "chemical hypoxia" in cultured cells to simulate the ATP depletion that occurs in ischemia (Herman et al., 1990; Sen et al., 1988; Sun et al., 1993). The observed biochemical, functional, and morphological changes occurring in the IAA-induced cell injury process compare favorably with the pathology of brain cells suffering hypoxic or ischemic injuries (Raichle, 1983). In this study, we used a moderate amount of IAA (75 μM) to generate a slowly evolving sequence of changes in human astrocytoma cells, so that we could examine the membrane structural changes in detail with fluorescence microscopy and elucidate the roles of these changes in the cell injury process. The data demonstrate that exposure of cells to IAA induces a slow decrease in the packing order of the lipid domains in the human astrocytoma cells during the first 70 min after the addition of IAA, which is followed by a rapid loss of lipid order. This phenomenon was evidenced both by the changes in r and by the changes in NBD-PC diffusion coefficient, as revealed by FRAP measurements. The results also confirm the postulation that an inverse relationship exists between r and the diffusion coefficient of fluorescent probes in the same system (Steiner, 1991).

A study of membrane structure changes during "chemical hypoxia" (high levels of IAA and KCN)-induced cell injury in cultured hepatocytes was reported by Wang et al. (1993), utilizing fluorescence quenching and fluorescence resonance energy transfer to measure lipid packing order. In contrast to the results reported here, which measure mem-

brane mobility, their results indicate an increase in lipid order as the hypoxic injury progressed; however, the hepatocytes develop large membrane blebs during the period of severe metabolic deprivation (no large bleb formation was observed in the astrocytoma cells utilized in our study) in which the membrane remained more fluid in nature. It is difficult to equate the two models; however, it is clear that changes in membrane structure are central to the hypoxic injuries observed in both models.

Many factors could account for the increase in the membrane fluidity during this cell injury process. One possibility is the peroxidation of membrane phospholipids induced by reactive oxygen species generated in traumatic or ischemic cell injury processes. We recently demonstrated the generation of reactive oxygen species in the IAA-induced cell injury in human astrocytoma cells using epifluorescence microscopy (Taylor et al., 1994). In that study, the generation of reactive oxygen species in the injured cells started 20 min after the exposure to IAA and reached a peak by 70 min, immediately before the loss of cell membrane integrity. This time course is consistent with the cell viability data reported here, where propidium iodide was used as a probe, and with the progression of membrane structural changes observed in the present study. Furthermore, the pretreatment of human astrocytoma cells with lipophilic antioxidants such as gossypol or tirilazad prevented the IAA-induced generation of reactive oxygen species and delayed lethal cell injury for a period of time (Taylor et al., 1994). Similar results have been reported in the other cell systems (Braughler and Hall, 1989; Hall and Braughler, 1989).

Gossypol is a naturally occurring component of cottonseed oil. It is a powerful lipophilic antioxidant (Knych, 1992) in different cell systems. When astrocytoma cells were treated with gossypol, the steady-state fluorescence anisotropy slightly decreased before reaching a constant level, which was not significantly different from the original value ($t = 0$). This slight decrease was probably due to the dynamic incorporation of gossypol molecules into the cell membranes. Similarly, the NBD-PC diffusion coefficient measured by FRAP was altered immediately after the addition of gossypol, indicating a slight alteration in the cell membrane upon incorporation of gossypol into the lipid bilayer. In IAA-treated cells, gossypol eliminated the dramatic decrease in r induced by IAA in unprotected cells. In addition, NBD-PC diffusion coefficients remained constant in gossypol-pretreated cells during IAA-induced injury. Together, these observations indicate that gossypol may substantially prevent IAA-induced membrane structural changes because of its antioxidant action.

Tirilazad is a compound belonging to the lazaroid series of lipophilic antioxidants developed to treat tissue injuries in the central nervous system originating from trauma or stroke. It was designed to distribute into the hydrophobic region of cell membranes to inhibit lipid peroxidation (VanGinkel et al., 1992; Audus et al., 1991; Braughler et al., 1989; Hall and Travis, 1988). In a biological membrane, tirilazad does not interact with the fluorescent probes (Audus et al., 1991), and therefore, all of the changes observed via the measurements of steady-state fluorescence anisotropy and FRAP can be interpreted as alterations in membrane structures. We found that r in the cells treated with tirilazad increased to a maximum in 30 min, although these changes were not observed in the cells treated with gossypol. Tirilazad also decreased the diffusion coefficient of the fluorescent probe in pretreated cells as measured in the FRAP experiments. These results not only illustrate the inverse relationship between r and membrane fluidity, but also suggest that tirilazad increases the lipid order of cell membranes. It should be noted that a previous report by Audus et al. (1991) also concluded that tirilazad increased the membrane lipid order in brain microvascular endothelial cells. In ATP-depleted cells, the decrease in r and the increase in the diffusion coefficient induced by IAA were both prevented by the pretreatment of cells with tirilazad. These results demonstrate that tirilazad may attenuate the structural damages of membranes occurring in the ischemic cell injury process, which in turn prolongs cell life.

Based on these results, we postulated that lipophilic antioxidants protect cells from irreversible injury via two mechanisms. They can protect cells 1) by quenching damaging reactive oxygen species and 2) by reinforcing the membrane structure and conferring resistance to damaging agents by changing membrane lipid structures.

In summary, we reported here the establishment of a method to measure the steady-state fluorescence anisotropy with the unique advantage of simultaneously monitoring both the vertical (parallel) and the horizontal (perpendicular) polarized fluorescence emissions needed to calculate r. This type of measurement, in combination with FRAP measurements, can be useful in investigating the changes of membrane structures occurring during the cell injury process induced by ATP depletion in human astrocytoma cells. With these techniques, we detected that r of the cell membranes decreased continuously after the loss of cellular ATP, indicating a decrease in membrane lipid order and perturbation of the bilayer structure. This decrease in r was prevented when the cells were pretreated with the lipophilic antioxidants. We suggest that the lipophilic antioxidants may protect the cells by increasing lipid order in the cell membranes and that the rigid membrane structure may contribute to the resistance against assaults by reactive oxygen or by autolytic enzymes during the process of irreversible cell injury.

The authors are very grateful to Dr. Melinda K. Frame of Meridian Instruments for her critical suggestions, Dr. Thomas J. Raub for providing the cell line, and to Dr. Dennis E. Epps for his help in measuring fluorescence anisotropy with the spectrofluorometer.

REFERENCES

Audus, K. L., F. L. Guillot, and J. M. Braughler. 1991. Evidence for 21-aminosteroid association with the hydrophobic domains of brain microvessel endothelial cells. *Free Radic. Biol. Med.* 11:361–371.

Axelord, D., D. E. Koppel, J. Schlessinger, E. Elson, and W. W. Web. 1976. Mobility measurements by analysis of fluorescence photobleaching recovery kinetics. *Biophys. J.* 16:1055–1069.

Braughler, J. M., and E. D. Hall. 1989. Central nervous system trauma and stroke. I. Biochemical considerations for oxygen radical formation and lipid peroxidation. *Free Radic. Biol. Med.* 6:289–301.

Braughler, J. M., E. D. Hall, E. J. Jacobsen, J. M. McCall, and E. D. Means. 1989. The 21-aminosteroids: potent inhibitors of lipid peroxidation for the treatment of central nervous system trauma and ischemia. *Drugs Future.* 14:143–152.

Brodie, A. E., and D. J. Reed. 1987. Reversible oxidation of glyceraldehyde 3-phosphate dehydrogenase thiols in human lung carcinoma cells by hydrogen peroxide. *Biochem. Biophys. Res. Commun.* 148:120–125.

Collins, J. M., and W. M. Grogan. 1989. Comparison between flow cytometry and fluorometry for the kinetic measurement of membrane fluidity parameters. *Cytometry.* 10:44–49.

Dawson, T. L., G. J. Goes, A. L. Nieminen, B. Herman, and J. J. Lemasters. 1993. Mitochondria as a source of reactive oxygen species during reductive stress in rat hepatocytes. Am. J. Pathol. 264:C961–C967.

Dix, J. A., and A. S. Verkman. 1990. Mapping of fluorescence anisotropy in living cells by ratio imaging: application to cytoplasmic viscosity. *Biophys. J.* 57:231–240.

el Hage Chahine, J. M., S. Cribier, and P. F. Devaux. 1993. Phospholipid transmembrane domains and lateral diffusion in fibroblasts. *Proc. Natl. Acad. Sci. USA.* 90:447–51.

Farber, J. L., K. R. Chien, and S. Mittnacht, Jr. 1981. The pathogenesis of irreversible cell injury in ischemia. *Am. J. Pathol.* 102:271–281.

Florine-Casteel, K., J. J. Lemasters, and B. Herman. 1991. Lipid order in hepatocyte plasma membrane blebs during ATP depletion measured by digitized video fluorescence polarization microscopy. *FASEB J.* 5:2078–2084.

Fushimi, K., J. A. Dix, and A. S. Verkman. 1990. Cell membrane fluidity in the intact kidney proximal tubule measured by orientation dependent fluorescence anisotropy imaging. *Biophys. J.* 57:241–254.

Goes, G. J., A. L. Nieminen, K. E. Fleishman, T. L. Dawson, B. Herman, and J. J. Lemasters. 1988. Extracellular acidosis delays onset of cell death in ATP-depleted hepatocytes. *Am. J. Physiol.* 255:C315–C322.

Golan, D. E., C. S. Brown, C. M. L. Cianci, S. T. Furlong, and J. P. Caulfield. 1986. Schistosomula of *Schistosoma mansoni* use lysophosphatidylcholine to lyse adherent human red blood cells and immobilize red cell membrane components. *J. Cell Biol.* 103:819–828.

Gough, A. H., and D. L. Taylor. 1993. Fluorescence anisotropy imaging microscopy maps calmodulin binding during cellular contraction and locomotion. *J. Cell Biol.* 121:1095–1107.

Hall, E. D., and J. M. Braughler. 1989. Central nervous system trauma and stroke. II. Physiological and pharmacological evidence for involvement of oxygen radicals and lipid peroxidation. *Free Radic. Biol. Med.* 6:303–313.

Hall, E. D., and M. A. Travis. 1988. Inhibition of arachidonic acid induced vasogenic edema by the non-glucocorticoid 21-aminosteroid U-74006F. *Brain Res.* 451:350–352.

Herman, B., G. J. Gores, A. L. Nieminen, T. Kawanishi, A. Harman, and J. J. LeMasters. 1990. Calcium and pH in anoxic and toxic injury. *CRC Crit. Rev. Toxicol.* 21:127–148.

Jennings, R. B., and K. A. Reimer. 1981. Lethal myocardial ischemic injury. *Am. J. Pathol.* 102:241–255.

Jennings, R. B., K. A. Reimer, C. Steenbergen, Jr., and J. Schaper. 1989. Total ischemia. III. Effect of inhibition of anaerobic glycolysis. *J. Mol. Cell Cardiol.* 21(Suppl. 1):37–54.

Knych, E. T. 1992. Endothelium-dependent tolerance to ethanol-induced contraction of rat aorta: effect of inhibition of EDRF action and nitric oxide synthesis. *Alcohol Clin. Exp. Res.* 16:58–63.

Lakowicz, J. R. 1983. Principles of Fluorescence Spectroscopy. Plenum Press, New York.

Lakowicz, J. R., editor. 1991. Topics in Fluorescence Spectroscopy. Plenum Press, New York.

Nieminen, A. L., G. J. Goes, B. E. Wray, Y. Tanaka, B. Herman, and J. J. Lemasters. 1988. Calcium dependence of bleb formation and cell death in hepatocytes. *Cell Calcium.* 9:237–246.

Padieu, P., and W. F. H. M. Mommaerts. 1960. Creatine phosphoryl transferase and phosphoglyceraldehyde dehydrogenase in iodoacetate poisoned muscle. *Biochim. Biophys. Acta.* 37:72–77.

Pirolo, J. S., and D. G. Allen. 1986. Assessment of techniques for preventing glycolysis in cardiac muscle. *Cardiovasc. Res.* 20:837–844.

Raichle, R. B. 1983. The pathophysiology of brain ischemia. *Ann. Neurol.* 13:2–10.

Sawyer, W. H. 1988. Fluorescence spectroscopy in the study of membrane fluidity: model membrane systems. *In* Methods for Studying Membrane Fluidity. R. C. Alora, C. C. Curtain, and L. M. Gordon, editors. Alan R. Liss, New York. 161–191.

Schindler, M., and L. W. Jiang. 1987. Fluorescence redistribution after photobleaching as a tool for dissecting the control elements of nucleocytoplasmic transport. *Methods Enzymol.* 141:447–459.

Sen, A., J. C. Miller, R. Reynolds, A. Chang, Y. Kim, M. D. Gunn, L. M. Buja, and K. R. Chien. 1988. Inhibition of the release of arachidonic acid from membrane phospholipids in cultured neonatal ray myocardial cells during adenosine triphosphate depletion. *J. Clin. Invest.* 82:1333–1388.

Steiner, R. F. 1991. Fluorescence anisotropy: theory and applications. *In* Topics in Fluorescence Spectroscopy, Vol. 2. J. R. Lakowicz, editor. Plenum, New York. 1–52.

Sun, F. F., W. E. Fleming, and B. M. Taylor. 1993. Degradation of membrane phospholipids in the cultured human astroglial cell line UC-11 MG during ATP depletion. *Biochem. Pharmacol.* 45:1149–1155.

Taylor, B. M., Y. Wu, and F. F. Sun. 1994. The effect of lipophilic antioxidants on the physiological changes occurring in ATP depletion induced lethal cell injury: a fluorescence analysis. *FASEB J.* 8:A408.

Taylor, D. L., and Y. L. Wang, editors. 1989. Methods in Cell Biology, Vol. 30. Academic Press, San Diego, CA.

van Ginkel, G., J. M. Muller, F. Siemsen, A. A. van 't Veld, L. J. Korstanje, and M. A. M. van Zandvoot. 1992. Impact of oxidized lipids and antioxidants, such as vitamin E and Lazaroids, on the structure and dynamics of unsaturated membranes. *J. Chem. Soc. Faraday Trans.* 88:1901–1912.

Wang, X. F., K. Florine-Casteel, J. J. Lemasters, and B. Herman. 1995. Video fluorescence microscopic techniques to monitor local lipid and phospholipid molecular order and organization in cell membranes during hypoxic injury. *J. Fluoresc.* 5:71–84.

Wang, X. F., J. J. Lemasters, and B. Herman. 1993. Plasma membrane architecture during hypoxic injury in rat hepatocytes measured by fluorescence quenching and resonance energy transfer imaging. *Bioimaging.* 1:30–39.

Wang, Y. L., and D. L. Taylor, editors. 1989. Methods in Cell Biology. Vol. 29. Academic Press, San Diego, CA.

Wu, Y., B. M. Taylor, and F. F. Sun. 1993. Cell membrane fluidity changes during early cell injury measured by fluorescence anisotropy imaging. *Mol. Biol. Cell.* 4:87A.